PERGAMON

International Journal of Heat and Mass Transfer 45 (2002) 4181–4190

International Journal of HEAT and MASS TRANSFER

www.elsevier.com/locate/ijhmt

Experimental and numerical investigation of the steady periodic solid–liquid phase-change heat transfer

Giovanni Casano [a], Stefano Piva [b,*]

[a] *Dipartimento di Ingegneria Energetica, Nucleare e del Controllo Ambientale, Università di Bologna, viale Risorgimento n. 2, 40136 Bologna, Italy*

[b] *Dipartimento di Ingegneria, Università di Ferrara, via Saragat n. 1, 44100 Ferrara, Italy*

Received 16 August 2001; received in revised form 27 February 2002

Abstract

A numerical and experimental investigation is presented of a periodic phase-change process dominated by heat conduction. In the experimental arrangement a plane slab of PCM is periodically heated from above. A one-dimensional control volume computer code has been developed for the solution of the corresponding mathematical model. The comparison between numerical predictions and experimental data shows good agreement, even though appreciable effects are produced by free convection and heat transfer to the environment, neglected in the model but unavoidable in the experiment. Finally, in order to study the energy stored in the process, parameters like amplitude and mean value of the oscillations are discussed as functions of the significant dimensionless numbers of the problem.

Keywords: Energy storage; Phase-change; Steady periodic heating

1. Introduction

Among the available techniques suitable for storing thermal energy and for controlling temperature in systems subjected to periodic heating, use of the solid–liquid phase-change has attracted considerable attention. This process allows, for periodic heating, the conversion of temperature oscillations into oscillations of the melting interface, with a significant damping of the perturbations. Furthermore, the energy stored during melting can be recovered during freezing, with significant energetic opportunities. Possible applications of engineering interest deal with a wide range of technologies, for instance steel industry, ground freezing, solar energy storage, thermal control systems for spacecraft and industrial waste heat recovery.

For the theoretical analysis of a melting phenomenon simultaneous solution is needed of the Fourier equation in the solid phase and of the mass, momentum and energy equations in the liquid phase, coupled by proper boundary conditions at the solid–liquid interface. This problem displays certain features that make the treatment particularly difficult. Even if natural convection is neglected, during the phase-change process the interface between the two phases moves and its position is *a priori* unknown. This makes the mathematical model strongly non-linear. Further difficulties arise when two-dimensional and three-dimensional geometries are considered or temperature-dependence of the thermophysical properties is taken into account. For all these reasons, only a limited number of analytical solutions for particularly simple cases exist, and for predictions of practical interest the use of numerical methods is required.

In the literature Bransier [1] seems to be the first who studied a system undergoing alternate processes of melting and freezing. He analysed the problem of cyclic latent heat thermal storage both for slabs and hollow cylinders, by means of a one-dimensional conduction

* Corresponding author. Tel.: +39-0532-974909; fax: +39-51-2090537.

E-mail address: piva@ing.unife.it (S. Piva).

0017-9310/02/$ - see front matter
PII: S0017-9310(02)00122-9

Nomenclature

A	amplitude of the energy oscillations (kJ/m^2)
A^*	dimensionless amplitude ($A/(q_0P/2\pi)$)
c	specific heat (kJ/kg K)
E	energy (kJ/m^2)
E_m	mean value of the energy oscillations (kJ/m^2)
E_m^*	dimensionless mean value of the energy oscillations ($E_m/(q_0P/2\pi)$)
f	initial temperature distribution (°C)
Fo	Fourier number
H	thickness of the specimen (m)
P	period (s)
q_H	reference heat flow (W/m^2)
r	latent heat of fusion (kJ/kg)
Ste	Stefan number
t	time (s)
T	temperature (°C)
t_r	time delay, Eq. (16)
T_R	reference temperature (q_0H/λ_s)
t_φ	time delay, Eq. (15)
x	axial coordinate (m)

Greek symbols

α	thermal diffusivity (m^2/s)
A	dimensionless thermal diffusivity (α_l/α_s)
φ	dimensionless initial temperature
λ	thermal conductivity (W/m °C)
Λ	dimensionless thermal conductivity (λ_l/λ_s)
η	amplitude reduction
θ	dimensionless temperature ($(T - T_f)/T_R$)
ρ	density (kg/m^3)
τ	dimensionless time (t/P)
ξ	dimensionless axial coordinate (x/H)
ω	pulsation (rad^{-1})
X	interface position (m)
Ξ	dimensionless interface position (X/H)

Subscripts

e	external
f	melting
in	introduced
H	at $x = H$
l	liquid
out	extracted
R	reference
s	solid
SPS	steady periodic state
t	total
0	at $x = 0$

model. Bardon et al. [2] performed the first experimental study on the periodic heat transfer for a vertical slab of PCM. Kalhori and Ramadhyani [3] investigated experimentally cyclic solid–liquid phase-change with finned and unfinned vertical cylinders embedded in *n*-eicosane. Jariwala et al. [4] studied the cyclic thermal performance of a latent heat thermal storage system obtained from a cylindrical container filled with a commercial paraffin wax, in which a helical pipe of copper was embedded. The results of a quasi-steady one-dimensional model developed for the purpose were in good agreement with the experimental data for energy storage and recovery. Sasaguchi and Viskanta [5] studied experimentally the effects of free convection on the periodic melting and freezing of pure *n*-octadecane around two cylindrical pipes spaced vertically. Adebiyi [6] carried out a second-law analysis on a packed bed storage system utilising phase-change materials. Bellecci and Conti [7–9] developed a numerical model to simulate the cyclic behaviour of a phase-change solar energy storage system. Using this model they expressed a criterion for the optimal design of such a storage system. Hasan et al. [10] investigated numerically and experimentally the conduction controlled periodic melting and freezing of a plane slab due to a thermal boundary condition cycling above and below the melting point. This investigation was extended by Voller et al. [11] taking into account the fluid motion in the liquid phase. Ghasemi and Molki [12], taking the analysis further, investigated numerically the effect of a thermal boundary condition cycling above and below the solidus temperature on the melting and solidification of steel in a rectangular enclosure. This, therefore, was able to include the two-phase "mushy" region at the liquid/solid interface.

A new trend in the utilisation of latent heat for the energy storage was started by Gong and Majumdar [13] using composite slabs consisting of PCMs with different melting points, but such an approach will not be examined in this work.

In order to provide further knowledge about the steady periodic heat transfer during cyclic processes of melting and freezing, in the present paper the problem has been analysed both numerically and experimentally. This can be considered as a development of the work of Hasan et al. [10]; in the present study the boundary condition of temperature cycling above and below a fixed melting temperature [10] is changed in a sinusoidal varying heat flux and the solid phase is significantly subcooled.

The investigation is limited to a one-dimensional case with negligible free convection effects. In the experiment, to prevent the possibility of natural convection in the

liquid phase, the sample, consisting in a solid slab of *n*-octadecane (n-$C_{18}H_{38}$), is placed horizontally and the heat transfer is directed vertically downward. The side wall is heavily thermally insulated. While the temperature at the base is kept uniform and lower than the melting point, a sinusoidal heat flow is supplied from above. During the evolution of the process, the temperature inside the octadecane is measured *via* thermocouples.

The numerical analysis provides results obtained by means of a control volume computer code developed specially for this work. Firstly, in order to verify the simplifying hypotheses of the theoretical model, a comparison between experimental data and numerical results is made. Then, the numerical approach is utilised to analyse the dependence of heat exchanged in the process on the significant dimensionless parameters. Specifically, the analysis focuses on the roles of the Stefan and Fourier numbers on the heat storage.

2. Experimental equipment and test procedure

A schematic diagram of the experimental equipment is shown in Fig. 1. The test cell consists of a polycarbonate round duct (outer diameter 150 mm, inner diameter 140 mm and height 210 mm) filled with the phase-change medium. Its bottom extremity is glued on a circular aluminium plate, used as the base. Such a base is kept at a temperature lower than the melting point of the test material by means of a refrigeration system. The uniform contact between the base and the refrigerator is enhanced by a thin layer of thermal conductive paste.

To remove easily the heat flow during the experiment, the refrigeration system uses Peltier cells. A uniform distribution of temperature over the whole surface of the bottom wall is obtained by means of nine thermoelectric modules (dimension $40 \times 40 \times 4$ mm^3) connected in series. They are sandwiched between a square plate of aluminium (2 mm of thickness) and a finned one

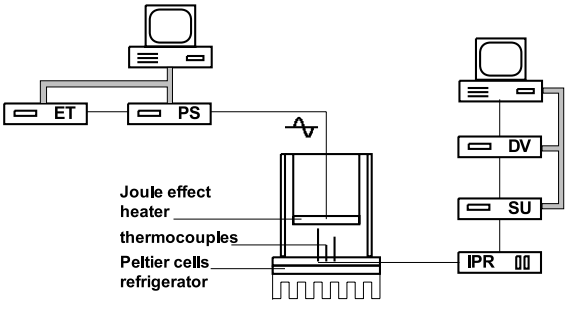

Fig. 1. Schematic diagram of the experimental equipment: ET, external trigger; PS, power supply; IPR, ice point reference; SU, switch control unit; DV, digital voltmeter.

(40 mm high fins). Uniform contact between the Peltier cells and the two aluminium plates is again enhanced by thin layers of thermal conductive paste. To facilitate the heat release by the thermoelectric refrigerator, the fins are immersed in a constant temperature bath, where the water is continuously stirred. The thermoelectric modules are supplied by direct current, choosing the polarity so as to give the cold surface on the test section and the hot one on the heat sink. The stability of the voltage supplied to the thermoelectric modules is guaranteed to within $\pm 1\%$.

In order to reduce the heat transfer to the environment, the wall of the cylinder is insulated with a 20 mm thick layer of foam rubber surrounded by a 100 mm thick layer of expanded polystyrene.

The test volume (height 51.1 mm) is closed on the top by the heater. The heat flow is obtained by dissipating via the Joule effect an assigned power in a resistor (450 W of nominal power at 220 V). Such a resistor is placed inside a copper disk soldered at the end of a cylindrical copper container (outer diameter 135 mm, inner diameter 133 mm and height 112 mm). This copper cylinder is placed coaxially inside the polycarbonate container. The air space between the two cylindrical surfaces is used as an auxiliary volume of expansion, allowing the volume of the liquid phase to change during the melting process.

The temperature inside the specimen is measured by copper–constantan thermocouples distributed at different heights. The positions of the thermocouples are shown in Table 1. The first and last thermocouples are in contact, respectively, with the hot and cold walls.

The hot junctions of the thermocouples are supported by polycarbonate stands. These prismatic supports (3 mm of side width) guarantee the positions of the thermocouples that in previous arrangements were uncertain, being affected by the dragging of the solid during the freezing. The wires leave the rigid supports through holes and grooves made in the bottom wall of the test cell.

A digital multimeter Hewlett–Packard HP3458A is used to measure the electromotive force for each thermocouple. The scanning of the thermocouples during the acquisition is carried out viaa switch control unit Hewlett–Packard HP3488A. The data acquisition system is managed through a personal computer IBM PS2/30 by means of an IEEE488 standard interface. The reference joint of the thermocouples is connected to an ice-point reference KAYE model K170, and the time is

Table 1
Positions of the thermocouples

TC no.	1	2	3	4	5	6	7	8
x (mm)	0	6.6	14.4	20.8	25.7	35	44.9	51.1

The origin is placed on the top of the specimen.

measured with the inner clock of the personal computer. The measured e.m.f. is converted into temperature using a third degree polynomial, the interpolation coefficients being computed on the basis of the ASTM temperature–e.m.f. tables for standardised thermocouples [14].

The test material is 99% pure *n*-octadecane, because it is non-corrosive and non-toxic, chemically inert and stable, with low vapour pressure, small volume changes during melting and large enthalpy release during the phase transition. The *n*-octadecane does not undergo any hysteresis cycle and its density decreases regularly as the temperature increases. Furthermore, its thermophysical properties are well known from the literature [15].

The sample is heated via resistance heating in a resistor, with the electric power sinusoidally varying in time. This power is obtained by varying the voltage *via* a programmable power supply Hewlett–Packard model HP6032A driven by a personal computer with an IEEE488 standard interface. The stability of the period is guaranteed by an external triggering, obtained with a signal generator Philips PM5192.

The melting temperature of the PCM has been measured to be $T_f = 28.0$ °C, which agrees with published data [15]. Since *n*-octadecane possesses a high capacity to absorb dissolved air, before each experiment the gas dissolved has been removed with heating and cooling cycles, carried out keeping the material under vacuum until bubble formation ceased. The pressure during the preparation of the test material was about 0.2 bar.

3. Mathematical formulation and numerical solution

The physical system consists of a horizontal plane slab of phase-change material. For thermal boundary conditions, at the bottom surface there is an assigned temperature and at the top wall an assigned uniform heat flux. When making comparisons with experimental data, however the top wall is kept at the measured temperature.

The mathematical model formulated to represent the physical system is based on the following simplifications:

- the PCM is homogeneous and isotropic;
- the thermophysical properties are constant in each phase;
- the phase-change occurs at a single temperature;
- the heat transfer is controlled only by conduction;
- the problem is one-dimensional;
- the difference of density between solid and liquid does not create appreciable local motion of the liquid.

The problem is then governed by the Fourier equation, to be solved for the two phases, solid and liquid

$$\frac{\partial T}{\partial t} = \alpha \frac{\partial^2 T}{\partial x^2} \tag{1}$$

The initial condition is given by

$$T(x, t = 0) = f(x) \tag{2}$$

The boundary conditions are given by

- cold surface

$$T(x = 0, t) = T_0(t) \tag{3}$$

- hot surface (assigned temperature)

$$T(x = H, t) = T_H(t) \tag{4.1}$$

- hot surface (assigned heat flow)

$$-\lambda \frac{\partial T}{\partial x}\bigg|_{x=H} = q_H \left[1 + \cos\left(\frac{2\pi}{P} t\right)\right] \tag{4.2}$$

At the phase-change interface two further conditions must be satisfied

$$\left[\lambda_s \frac{\partial T_s}{\partial x} - \lambda_l \frac{\partial T_l}{\partial x}\right]_{x=X} = \rho_s r \frac{dX}{dt} \tag{5}$$

$$T_s = T_l = T_f \tag{6}$$

Eqs. (5), (6) are those typical of the Stefan problem. These consider the release or the storage of energy during the freezing or melting; generally the interface position is unknown a priori.

Eqs. (1)–(6) have been made dimensionless in order to individualise the significant parameters of the problem; the non-dimensional variables are defined as follows:

$$\vartheta = \frac{T - T_f}{T_R} \quad \tau = \frac{t}{P} \quad \xi = \frac{x}{H}$$

The reference temperature is $T_R = (q_H H)/\lambda_s$

In terms of dimensionless variables Eqs. (1)–(6) can be written as

- Solid phase

$$\frac{\partial \vartheta}{\partial \tau} = Fo \frac{\partial^2 \vartheta}{\partial \xi^2} \tag{7}$$

- Liquid phase

$$\frac{\partial \vartheta}{\partial \tau} = AFo \frac{\partial^2 \vartheta}{\partial \xi^2} \tag{8}$$

- Solid–liquid interface

$$\left[\frac{\partial \vartheta_s}{\partial \xi} - \Lambda \frac{\partial \vartheta_l}{\partial \xi}\right]_{\xi=\Xi} = \frac{1}{Ste \cdot Fo} \frac{d\Xi}{d\tau} \tag{9}$$

$$\vartheta_s(\xi = \Xi) = \vartheta_l(\xi = \Xi) = 0 \tag{10}$$

- Initial condition

$$\vartheta(\xi, \tau = 0) = \varphi(\xi) \tag{11}$$

- Boundary conditions

cold surface

$$\vartheta(\xi = 0, \tau) = \vartheta_0(\tau) \tag{12}$$

hot surface (assigned temperature)

$$\vartheta(\xi = 1, \tau) = \vartheta_H(\tau) \tag{13.1}$$

hot surface (assigned heat flow)

$$-\Lambda \frac{\partial \vartheta}{\partial \xi}\bigg|_{\xi=1} = 1 + \cos(2\pi\tau) \tag{13.2}$$

The significant dimensionless parameters of the problem are as follows:

$$Fo = \frac{\alpha_s P}{H^2} \quad Ste = \frac{T_R c_s}{r} \quad A = \frac{\alpha_l}{\alpha_s} \quad \Lambda = \frac{\lambda_l}{\lambda_s}$$

$$\vartheta_0 = \frac{T_0 - T_f}{T_R} \quad \varphi = \frac{f(x) - T_f}{T_R}$$

In general, the Stefan Eqs. (5), (6) introduce a strong non-linear character into the differential problem precluding any analytical solution, especially for complex configurations. Therefore, it is essential to use of a numerical approach.

The present one-dimensional problem has been treated numerically using the control volume method [16]. To search for the phase-change interface, a front tracking, time explicit scheme is adopted [17]. Control volumes of uniform size and constant time steps are used. To initialise the phase-change, the first advance is calculated by a linear interpolation. The numerical technique is quite standard; further details are available in [17].

Beside the temperature distribution, the energy stored per unit area is also calculated. The cumulative energy introduced in the system up to time t through the boundary condition Eq. (4.2) is

$$E_{in}(t) = q_H t + \frac{q_H P}{2\pi} \sin\left(\frac{2\pi}{P} t\right) \tag{14}$$

In the discussion of the results, the amplitude and the mean value of the energy stored in the system are made dimensionless by dividing by $q_H P/2\pi$. The latter is the amplitude of the energy supplied in a cycle, Eq. (14).

4. Numerical code validation

When the free surface of a liquid and isothermal semi-infinite layer is moved to a temperature lower than the melting point, the temperature distribution and the interface position can be calculated analytically [18]. For such a case a comparison exercise between numerical and theoretical results may be arranged in order to evaluate the reliability of the numerical approach. For this comparison the value of the parameters are those used by Comini et al. [19], who chose water as the working fluid.

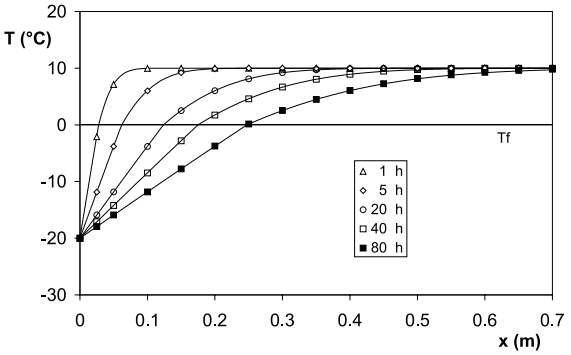

Fig. 2. Validation test: comparison between numerical and analytical temperature distributions (lines: numerical results, symbols: analytical results).

When using the computer code for the analysis of the semi-infinite layer, the domain needs to be limited to a finite depth ($L = 1$ m) where a condition of assigned temperature is set. The computation is then terminated when the phase-change front reaches a position such to produce a significant heat flux at the "infinite–finite" cut-off domain.

In the validation exercise the comparison is carried out for the following parameters: temperature, interface position and energy exchanged in the solidification process.

In Fig. 2 the calculated temperature distributions at five different times are compared with the analytical solution. The grid size ($\Delta x = 1.25$ mm) and the corresponding time step ($\Delta t = 0.5$ s) guarantee the stability of the computation. It is evident that the agreement between numerical and analytical results is excellent. The effect of the boundary condition imposed at $x = L$ becomes sensible only after almost 80 h.

5. Results and discussion

5.1. Numerical–experimental comparison

Having demonstrated the numerical validity of the code by comparison with results for an analytical solution (Section 4), the physical validity of the mathematical model may be studied by comparison of predictions with experimental data.

The experimental tests were carried out so as to obtain cyclic processes of melting and freezing in a sample of *n*-octadecane. The experiments always included a preliminary settling period when the sample, previously frozen in a refrigerator, was kept solid. When the measured temperature of the sample became practically

uniform, enabling the reaching of steady-state conditions to be assured, the heating system was activated and the periodic heating process started.

The results of the comparison are reported for three experimental tests. The runs differ according to the period of the sinusoidal power dissipated in the heater (4, 8 and 16 h for Test a, b and c respectively). The temperature was sampled every 4 min, the experiments lasting for 24 h in the case of Test a and 48 h for Tests b and c.

For these trials a numerical simulation was carried out by using the measured top and bottom temperature as the boundary conditions. A linear interpolation of the sampled data was used to calculate the boundary values needed in the computation but not available experimentally. The effect of this simplification on the numerical solution is negligible. A uniform grid of 257 control volumes ($\Delta x = 0.2$ mm) was used, together with a time step equal to $\Delta t = 0.2$ s, necessary to satisfy the stability condition.

In Fig. 3, for the selected runs, the measured and computed temperature distributions are compared. Results for the three tests show that only Test b reaches steady periodic conditions; Tests a and c are too short for this steadiness to be achieved.

For all the tests reported in Fig. 3, the presence of an interface separating an upper zone, where the material is liquid, from a lower zone at the solid state, is clearly evidenced. The liquid zone is characterised by wide oscillations of temperature, reaching the maximum amplitude at the heated surface (equal to 5, 8 and 15 °C for Tests a, b and c respectively).

The solid region is characterised by moderate oscillations of temperature, practically negligible in Test a and increasing with the period. This is because the greater part of the heat flux introduced in the sample via the heater is used for the advancement of the interface and only a limited part of this flux is still available for the heating of the remaining solid.

In the experiments the coexistence of more phase-change surfaces was not detected, in contrast to that found by other authors [1,3,10,12]. This is due to the particular boundary condition adopted here, in that the heat flux is never extracted from the top surface and the solid phase is significantly subcooled at the beginning of the experiment.

In Fig. 3 the non-linear effect due to the Stefan condition is evident; while the oscillations of temperature seem to be sinusoidal when completely included in the liquid or in the solid phase, they change from this shape when intersecting the phase-change surface. In fact, they are clearly distorted, as particularly evident in Test b.

The comparison among the numerical and the experimental data is very good. The decision to neglect all phenomena but the conduction, as proposed by Hasan et al. [10] for a similar experimental arrangement but a different heating scheme, is confirmed by the excellent results. Again, then, the prevailing role is played by the conduction.

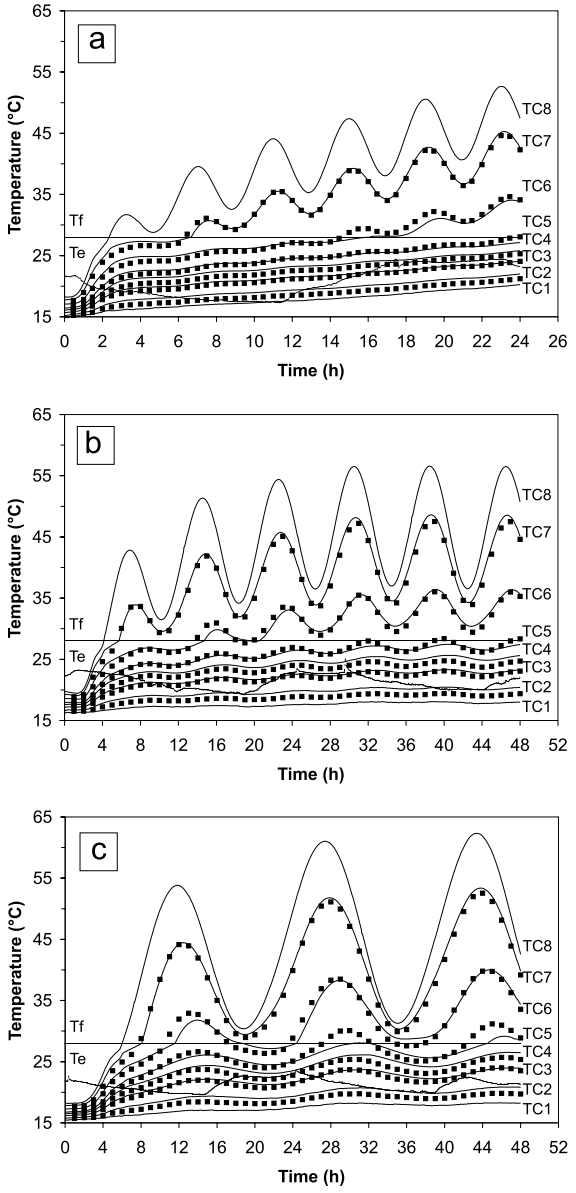

Fig. 3. Comparison between computed (lines) and measured (symbols) temperature distributions for tests of different periods (a: 4 h; b: 8 h; c: 16 h).

From a qualitative point of view the numerical model gives trends of temperature totally similar to those experimental, both in the solid and in the liquid phase. The start of the melting process, and of the following freezing and melting cycles, appears clearly and the wide oscillations of temperature in the liquid are also well evident.

From a quantitative point of view the comparison is also positive, with some significant differences in the solid phase, where the calculated temperature is appreciably higher than the experimental. Furthermore, the numerical model tends to give faster advance of the solid–liquid interface. This difference becomes more evident for increasing Fourier numbers.

The above observed quantitative disagreement can find a justification in the simplifying assumptions of the model. First of all a one-dimensional conduction model has been used to simulate what is a two-dimensional problem, where the convection, even though lowered by the choice of the material and of the manner of heating, is always present. The one-dimensional mathematical model excludes lateral heat exchange, which would tend to reduce the heat flow available at the interface, and therefore slow down the process. Furthermore, the lateral heat exchange, and therefore the lower values of temperature in the peripheral zones of the sample, can be the origin of convective motions. The effect of the convection is to increase the heat transfer on the lateral zone of the liquid phase and result therefore in a further slowing in the advance of the interface. It must be noted that for periodic heating the quantitative disagreement is less significant than for the case of constant heating [20].

5.2. Energy evaluations

Since both the numerical and the physical validations of the computer code are now positively demonstrated, the energy behaviour of this phase-change system has also been numerically analysed. Due to the complexity of the problem, which involves both sensible and latent heat transfer, the analysis is mainly focused on the role played by the significant dimensionless parameters.

For a case characterised by $Ste = 0.5$, $Fo = 4$, $\Lambda = 1$, $A = 1.17$ and $\vartheta_i = \vartheta_0 = -0.47$, the trends of total, sensible and latent energy stored and of the interface position are presented in Fig. 4 as a function of time. It is evident that, after an initial phase of sensible heating, the melting front moves until it oscillates steadily around a constant mean value. The total energy storage, steady periodic after only a few periods, seems to be sinusoidal and, for the following evaluations, has been interpolated as

$$E_t(t) = E_m + A \sin\left[\frac{2\pi}{P}(t - t_\varphi)\right] \tag{15}$$

Unlike the total storage, the sensible and latent heat storage show trends periodic but clearly not sinusoidal, lagging each other in time. A significant contribution to this phase shift is due to the preliminary sensible heating of the slab. This delays the beginning of the phase-change phenomenon, which starts only when the top surface reaches the phase-change temperature.

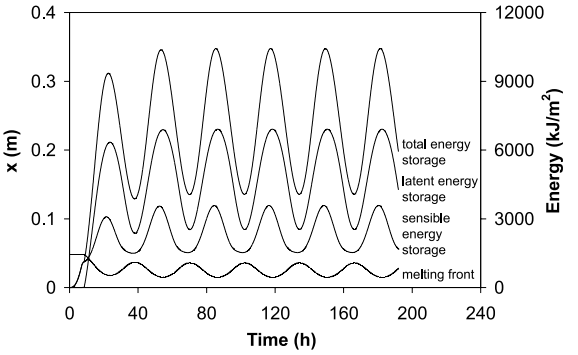

Fig. 4. Energy storage and interface position in the steady periodic heating.

In more depth, the analysis of the energy stored in the system shows that for the highest Fourier numbers the distribution diverges, even if marginally, from sinusoidal. For this reason in Eq. (15) the mean value of the energy stored over a period, E_m, is calculated separately in order to ensure that the same energy has been stored of the real distribution.

In Fig. 5 the dimensionless mean value, E_m^*, and amplitude, A^*, of the energy stored at the steady periodic state, Eq. (15), are reported as a function of the Fourier number, for several values of the Stefan number. All the data refer to the same dimensionless initial and bottom temperature, $\vartheta_i = \vartheta_0 = -0.47$, and to the following dimensionless properties of the PCM, namely $\Lambda = 1$ and $A = 1.17$.

The dimensionless mean value of the total energy stored in the system (Fig. 5a) shows a regular behaviour: for a fixed Stefan number it decreases as the Fourier number increases. If, instead, lines of constant Fourier number are plotted on an energy–Stefan number graph, precisely the same pattern would result. In a physical sense it means that for high frequencies of oscillation (low Fourier number values) or for high latent storage capabilities (small Stefan number values) at the periodic steady-state the mean value of the energy stored in the system can be great. Conversely, for the range of validity of the analysis, limited to values of the Stefan and Fourier numbers where simultaneous sensible and latent heat transfer occur ($E_m^* > 1$), either for large periods (high Fourier numbers), or for low latent storage capabilities (high Stefan numbers), the dimensionless mean energy stored tends to small values.

The dimensionless amplitude of the total energy stored in the system is shown in Fig. 5b. For small values of the Fourier number ($Fo \leqslant 0.125$) the dimensionless amplitude of the total energy stored (Fig. 5b) is constant and independent of the Stefan number. In particular, within this range the dimensionless amplitude is equal to unity. This means that the energy stored oscillates with

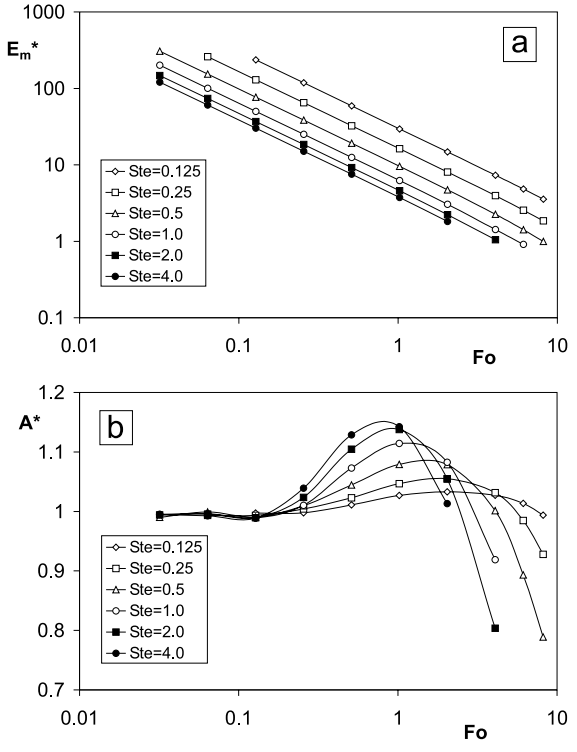

Fig. 5. Dimensionless mean value (a) and amplitude (b) of the oscillations of the total energy stored at the steady periodic state.

the same amplitude as the energy introduced, and that the entire oscillation of heat flux supplied is converted into an oscillation of the melting front. In this region the system behaves as a damper, because against an oscillating heat input (Eq. (4.2)), the flux emerging is constant (Fig. 6).

For higher values of the Fourier number ($Fo > 0.125$) the dimensionless amplitude of the total energy stored in the system begins to be influenced by the Stefan number. The heat flux emerging from the bottom surface begins to oscillate (Fig. 6). In this case for a fixed Stefan number the dimensionless amplitude attains a maximum (Fig. 5b). The position of this maximum occurs at reduced Fourier numbers, while its value increases with Stefan numbers. After the maximum, the dimensionless amplitude, A^*, decreases for increasing Fourier numbers at increasing rates as the Stefan number is increased. However, for small values of the Stefan number, the dimensionless amplitude of the oscillation of energy is less sensitive to the Fourier number and therefore to the period of the oscillation.

As a general comment, it can be observed that the dimensionless amplitude of the oscillations of energy stored becomes more sensitive to the Fourier number for the higher Stefan numbers, that is when the sensible

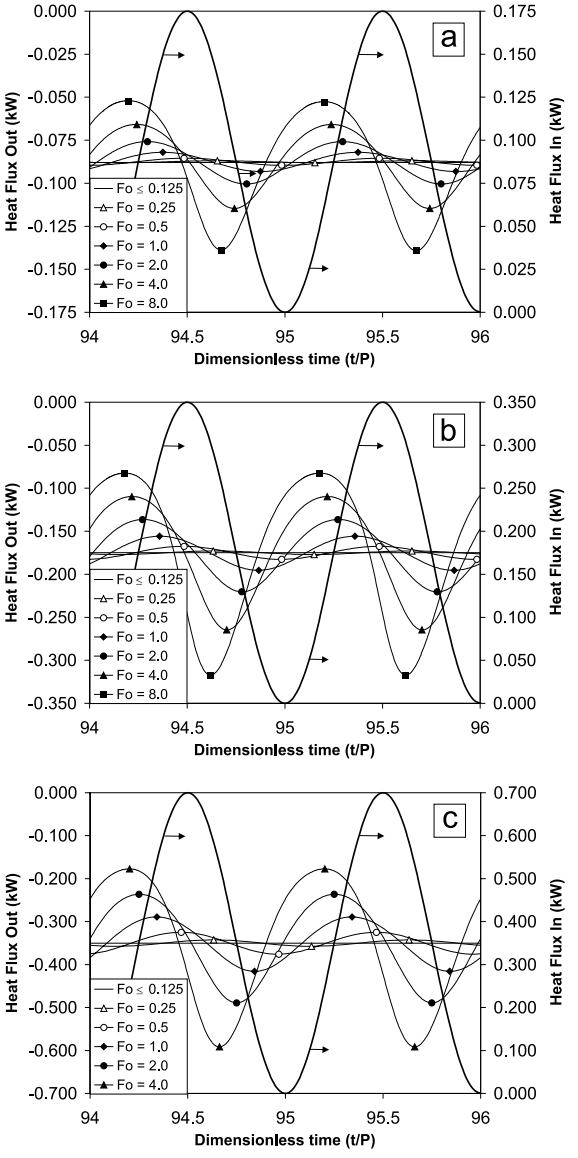

Fig. 6. Heat fluxes introduced and extracted from the boundary surfaces of the system after 94 periods when the steady periodic state is attained (a: $Ste = 0.25$; b: $Ste = 0.5$; c: $Ste = 1.0$).

heating becomes prevalent. When the oscillations are of long period (high Fourier numbers) the amplitude of the energy stored can be negligible. Conversely, when the oscillations are of short period (low Fourier numbers) the amplitude of the energy stored is practically constant and equal to the amplitude of the energy introduced into the system. This behaviour, and particularly the occurrence of a maximum higher than one, can be explained by considering that the energy storage is given by the time integral of the difference between the sinusoidal heat fluxes introduced, Eq. (4.2), and extracted, Fig. 6.

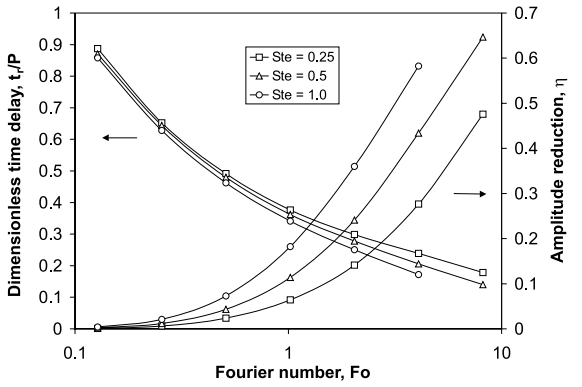

Fig. 7. Time delay and amplitude reduction of the heat fluxes extracted from the system.

The heat flux outgoing from the bottom surface shows, as well evident in Fig. 6, a reduced amplitude and a time delay changing with the Fourier and Stefan numbers, when compared to the entering heat flux. These two parameters, time delay t_r and amplitude reduction η, are obtained by interpolating the data of Fig. 6 with the following equation:

$$q_{out} = q_H\left[1 + \eta\cos\left(\frac{2\pi}{P}(t - t_r)\right)\right] \tag{16}$$

In Fig. 7 are shown the results of this interpolation for different values of the Fourier and Stefan numbers. In more detail, for a fixed Stefan number the amplitude increases and the phase shift reduces with the Fourier number.

Returning to the energy behaviour of the system (see Appendix A for full details) when subtracting two sinusoidal signals of the same pulsation but of different amplitude and phase (energy introduced and extracted), the amplitude of the resulting signal (energy stored) changes from the difference of the amplitudes for $t_r = P$ to their summation for $t_r = 0$. This enables the amplitude of the oscillations of the energy stored to be greater than that of the energy introduced into the system.

6. Concluding remarks

A numerical code has been developed for the analysis of cyclic one-dimensional phase-change in a slab which gives useful and reliable results. It enables all the information necessary to be obtained in studying the process, for which conduction is prevalent over the other heat transfer effects.

A comparison between experimental and numerical distributions of temperature gives very good results. In this comparison only minor discrepancies arise. When it is considered that in the experiment both free convection and heat transfer through the side wall of the specimen are small but not negligible, the results of the comparison serve to justify the assumptions made as the basis of the mathematical model.

The analysis of the energy behaviour of the system also gives interesting results. The energy stored in the system oscillates in time with the energy introduced. A regular behaviour is shown by dimensionless mean value of the energy stored, decreasing for increasing Fourier numbers and also for increasing Stefan numbers. For small values of the Fourier number the dimensionless amplitude of the oscillations of the energy stored in the system is constant, independent of the values of the Stefan number. In this case the system is able to act as a damper of entering energy oscillations and the heat flux emerging from the output surface is almost constant. Conversely, for increasing Fourier numbers the amplitude strongly depends on the Stefan number. Furthermore, the amplitude shows a maximum, which is more marked for large values of the Stefan number. It means that for large period of oscillation there are situations where the system does not exert any damping effect.

Acknowledgements

The authors thank Prof. Giorgio Pagliarini for the helpful discussions on this work.

Appendix A

The energy introduced into the system is given by Eq. (14)

$$E_{in}(t) = \int_0^t q_{in}(t)\mathrm{d}t = q_H t + \frac{q_H P}{2\pi}\sin\left(\frac{2\pi}{P}t\right) \tag{A.1}$$

When the steady periodic state is attained, it means after a certain time referred to as t_{SPS}, the heat flow outgoing from the bottom of the specimen is given by Eq. (16) and the energy released from the system is

$$E_{out,SPS}(t) = \int_{t_{SPS}}^t q_{out}(t)\mathrm{d}t = q_H(t - t_{SPS}) + \frac{\eta q_H P}{2\pi}\left[\sin\left(\frac{2\pi}{P}(t - t_r)\right) - \sin\left(\frac{2\pi}{P}(t_{SPS} - t_r)\right)\right] \tag{A.2}$$

The oscillating part of the energy stored by the system, Eq. (15), is given by the difference of the oscillating parts of Eqs. (A.1) and (A.2)

$$A\sin\left(\frac{2\pi}{P}(t-t_\varphi)\right)=\frac{q_H P}{2\pi}\left[\sin\left(\frac{2\pi}{P}t\right)-\eta\sin\left(\frac{2\pi}{P}(t-t_r)\right)\right] \quad (A.3)$$

Remembering that

$$X\sin(t+\alpha)+Y\sin(t+\beta)=S\sin(t+\varphi) \quad (A.4)$$

where

$$S^2=X^2+Y^2+2XY\cos(\alpha-\beta) \quad (A.5)$$

$$\tan\varphi=\frac{X\sin\alpha+Y\sin\beta}{X\cos\alpha+Y\cos\beta} \quad (A.6)$$

the amplitude of the oscillations of the energy stored becomes

$$A=\frac{q_H P}{2\pi}\sqrt{1+\eta^2-2\eta\cos\left(\frac{2\pi}{P}t_r\right)} \quad (A.7)$$

and their time delay

$$t_\varphi=\frac{P}{2\pi}\tan^{-1}\left(\frac{-\eta\sin\left(\frac{2\pi}{P}t_r\right)}{1+\eta\cos\left(\frac{2\pi}{P}t_r\right)}\right) \quad (A.8)$$

It is evident that the dimensionless amplitude of the oscillations of the energy stored can be $A^*=(1+\eta)$ if $t_r=P/2$ and $A^*=(1-\eta)$ if $t_r=0$, it means for low and high Fourier numbers respectively (Fig. 7).

References

[1] J. Bransier, Storage periodique par chaleur latente: aspects fondamentaux lies a la cinetique des transferts, Int. J. Heat Mass Transfer 22 (1979) 875–883.

[2] J.P. Bardon, E. Vrignaud, D. Delaunay, Etude expérimentale de la fusion et de la solidification périodique d'une plaque de paraffine, Rev. Gen. Therm. 212–213 (1979) 501–510.

[3] B. Kalhori, S. Ramadyani, Studies on heat transfer from a vertical cylinder with or without fins embedded in a solid phase change medium, J. Heat Transfer 107 (1985) 44–51.

[4] V. Jariwala, A.S. Mujumdar, M.E. Weber, The periodic steady state for cyclic energy storage in paraffin wax, Can. J. Chem. Eng. 65 (1987) 899–906.

[5] K. Sasaguchi, R. Viskanta, Phase change heat transfer during melting and resolidification of melt around cylindrical heat sources/sinks, J. Energy Resour. Technol. 111 (1989) 43–49.

[6] G.A. Adebiyi, A second-law study on packed bed energy storage systems utilising phase-change materials, J. Sol. Energy Eng. 113 (1991) 146–156.

[7] C. Belleci, M. Conti, Phase change thermal storage: transient behaviour analysis of a solar receiver/storage module using the enthalpy model, Int. J. Heat Mass Transfer 36 (1993) 146–156.

[8] C. Belleci, M. Conti, Transient behaviour analysis of latent heat thermal storage module, Int. J. Heat Mass Transfer 36 (1993) 2157–2163.

[9] C. Belleci, M. Conti, Latent heat thermal storage for solar dynamic power generation, Sol. Energy 51 (1993) 169–173.

[10] M. Hasan, A.S. Mujumdar, M.E. Weber, Cyclic melting and freezing, Chem. Eng. Sci. 46 (1991) 1573–1587.

[11] V.R. Voller, P. Felix, C.R. Swaminathan, Cyclic phase change with fluid flow, Int. J. Numer. Meth. Heat Transfer Fluid Flow 6 (1996) 57–64.

[12] B. Ghasemi, M. Molki, Cyclic melting and solidification of steel, Numer. Heat Transfer Part A 32 (1997) 877–896.

[13] Z. Gong, A.S. Mujumdar, Enhancement of energy charge–discharge rates in composite slabs of different phase change materials, Int. J. Heat Mass Transfer 39 (1996) 725–733.

[14] ASTM Standard E230-87, Temperature–electromotive force (EMF) tables for standardised thermocouples, 1987.

[15] W.R. Humphries, E.I. Griggs, A design handbook for phase change thermal control and energy storage devices, NASA Technical Paper, 1074 (1977).

[16] S.V. Patankar, Numerical heat transfer and fluid flow, Hemisphere, New York, 1980.

[17] G. Casano, Theoretical and experimental investigation on the thermal storage characteristics of phase-change systems, Ph.D. Thesis, Università di Bologna, Bologna, 1996 (in Italian).

[18] A.V. Luikov, Analytical Heat Diffusion Theory, Academic Press, New York, 1968.

[19] G. Comini, S. Del Giudice, R.W. Lewis, O.C. Zienkiewicz, Finite element solution of non-linear heat conduction problems with special reference to phase change, Int. J. Numer. Meth. Eng. 8 (1974) 613–624.

[20] M. Pinelli, G. Casano, S. Piva, Solid–liquid phase-change heat transfer in a vertical cylinder heated from above, Int. J. Heat Technol. 18 (2000) 61–68.